

TiEV: The Tongji Intelligent Electric Vehicle in the Intelligent Vehicle Future Challenge of China

Junqiao Zhao^{*,1,2}, Chen Ye^{1,2}, Yan Wu^{1,2}, Linting Guan^{1,2}, Lewen Cai^{1,2}, Lu Sun^{1,2}, Tao Yang^{1,2}, Xudong He^{1,2}, Jun Li^{1,2}, Yongchao Ding^{1,2}, Xinglian Zhang³, Xinchun Wang^{1,2}, Jinlin Huang^{1,2}, Enwei Zhang^{1,2}, Yewei Huang³, Wei Jiang^{1,2}, Shaoming Zhang³, Lu Xiong⁴ and Tiantian Feng³

Abstract—TiEV is an autonomous driving platform implemented by Tongji University of China. The vehicle is drive-by-wire and is fully powered by electricity. We devised the software system of TiEV from scratch, which is capable of driving the vehicle autonomously in urban paths as well as on fast express roads. We describe our whole system, especially novel modules of probabilistic perception fusion, incremental mapping, the 1st and the 2nd planning and the overall safety concern. TiEV finished 2016 and 2017 Intelligent Vehicle Future Challenge of China held at Changshu. We show our experiences on the development of autonomous vehicles and future trends.

I. INTRODUCTION

Autonomous driving has long been seen as one of the ultimate solutions to transportation problems like the traffic jam and traffic accidents [14], [15]. In the past decade, the well-known DARPA challenges had proved its possibility and demonstrated the technique frameworks [2], [15], [19]. Later led by universities as well as their industrial counterparts, autonomous driving researches have witnessed a dramatic growth [1], [4]–[6], [8], [17], [22]. The latest prototypes, such as Waymo, have already shown their capability of driving more safely than human beings [9], [20]. Nevertheless, in general, the autonomous driving technique is still in its infancy, especially when facing complex urban scenes where human drivers could easily interpret the traffic and act accordingly based on him/her experiences.

Sponsored by NSFC, China’s similar event, the Intelligent Vehicle Future Challenge (IVFC) began from 2009 [13]. In the last eight years, more than thirty universities, as well as companies, participated in the challenges, which is now recognized as the most influential event of the R&D of the autonomous driving in China. Tongji Intelligent Electric Vehicle (TiEV) project funded by the Tongji University was started in 2014. The aim of this project is to build an autonomous driving prototype that can cope with the complex urban driving scenarios based on cutting-edge AI technologies.

This work is supported by the National Natural Science Foundation of China (No. U1764261), the Natural Science Foundation of Shanghai (No.kz170020173571) and the Fundamental Research Funds for the Central Universities (No. 22120170232)

¹The Key Laboratory of Embedded System and Service Computing, Ministry of Education, Tongji University, Shanghai zhaojunqiao@tongji.edu.cn

²Department of Computer Science and Technology, School of Electronics and Information Engineering, Tongji University, Shanghai

³School of Surveying and Geo-Informatics, Tongji University, Shanghai

⁴School of Automotive Studies, Tongji University, Shanghai

TiEV is modified from an electric vehicle (Fig. 1). It is equipped with seven vision sensors, four laser sensors, and a GPS+IMU system. The computer systems are composed of two IPCs with quad-core CPU and one embedded system. The software of TiEV is distributed in three computers and implemented in a cross-platform environment. TiEV proposed novel modules of probabilistic perception fusion, incremental mapping, the 1st and the 2nd planning, which will be detailed in the following sections. The overall safety is of great importance in our systematic design. We could guarantee collision-free even if the wrong decision was made by the planning module. TiEV participated in 2016 and 2017 IVFC and successfully managed to pass most of the tasks.



Fig. 1. The TiEV autonomous driving platform

II. THE ARCHITECTURE

A. The vehicle

TiEV is modified from Rowe E50 of SAIC motors (Fig. 1). The car is a four seats two doors mini car of 3.569 meters long and 1.55 meters wide and fully driven by electricity. Its maximum range is 100 kilometers on a charge. The EPS and the motor can be controlled-by-wire through CAN. We install a parallel ABS system to enable the control-by-wire of the braking system.

Fig. 2 shows the overall architecture of the hardware system of TiEV. We equipped totally seven vision sensors. Two of the three forward-looking cameras compose a stereo vision system and the other is used for the detection task. The four fish-eye cameras are calibrated to compose a surround-vision system, which can provide a top-down panorama view of about 10 meters by 10 meters. The Velodyne

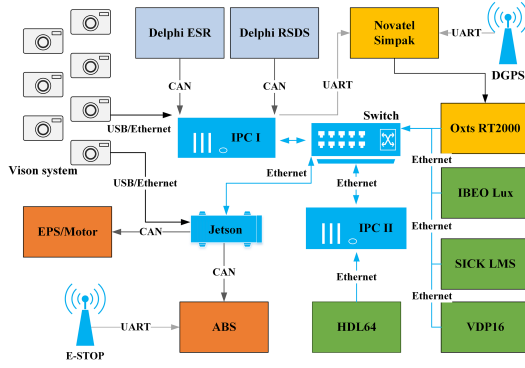


Fig. 2. The system architecture of TiEV

HDL64 is responsible for the segmentation of drivable area and the detection of moving obstacles such as pedestrians and vehicles. To complement the blind-area of HDL64, an IBEO Lux4 and a Sick LMS511 scanner are installed. Their positions can either be in the front or in the rear. A high precision GPS+IMU system integrated by Novatel simpak6 GPS receiver and Oxts RT2000 IMU provides accurate localization information of about 10 centimeters in the outdoor environment.

There are three computers installed on TiEV. Two of them are Advantech IPCs, and the other is an embedded system based on NVIDIA Jetson TX2. TX2 is equipped with a Pascal GPU and is capable of CAN communication. As a result, a camera and the CAN bus are linked to this computer, on which the deep learning module and CAN actuation module are implemented.

B. Modules overview

The software modules of TiEV are highly distributed, and communications between modules are decentralized. This flexible and robust structure has been adopted by many similar systems. We employed the popular LCM middleware [12], which is lightweight and supports cross-platform. The exact synchronization between modules is not required in our system. A spatiotemporal stamp is introduced for the fusion of asynchronous information. As a result, each module processes in its own operation cycle, which is constrained by the upstream and downstream modules.

Fig. 3 shows the software architecture and interactions between modules. Different colors indicate the different computers on which modules are implemented, i.e., gray indicates *IPC I*, orange indicates *IPC II* and green indicates *Jetson*. Messages can be categorized into four classes, which are grid-based *map*, tracked *objects*, detected *signal* and generated *trajectory*. The message of the spatiotemporal stamp is received by all modules. The following sections will describe the featured modules in our system.

III. PERCEPTION UNDER UNCERTAINTY

Perception is the basis for autonomous systems. Multiple sensor readings should be fused into a unified representation for decision-making. TiEV adopted a 2D grid-based representation for obstacles located within the decision region

(80 meters by 30 meters). However, sensor readings can be noisy thus we should fuse them in a probabilistic form. In this section, we will first address the modules for laser scanners and vision sensors. Then the fusion methods will be explained.

A. Laser perception

1) *Multibeam Laser*: This module processes the 3D point clouds send from HDL64. We implement obstacle segmentation, classification, and tracking consecutively.

The segmentation is conducted in two steps: Firstly, an up-sampled grid map¹ is used to classify obstacle points based on height differences. In the next step, we traverse the original grid map. The cell which contains obstacle points located within the vertical span of the vehicle is marked as an obstacle. Therefore flat surfaces such as car roofs can be preserved. In the meanwhile, we classify each of the obstacle clusters based on a classifier proposed in [18], which results in cars, bicycles, and pedestrians. Kalman filters are then created for each object to predict their movements in contiguous frames (Fig. 4).

2) *Sick and IBEO*: These sensors are mainly used as complements to HDL64, especially in the near and far front of the vehicle. We compensate the extrinsic parameters of both sensors based on *pitch* readings from IMU and project the points onto the grid map.

Afterwards, all the grid maps generated from laser perception modules will be fused in the *Fusion* module (Sec. III-C).

B. Visual perception

1) *Forward vision*: We get rich visual information from three Basler Ace cameras mounted behind the windshield and above the rear-view mirror of the vehicle. Two of them compose a stereo rig for depth vision (Fig. 5 a)) and the other is used for detection purpose. We trained a model based on YOLO2 to detect cars, pedestrians and traffic signs [16] (shown in Fig. 5 b)). 2D boxes of cars and pedestrians are further mapped to 3D point cloud in *Multibeam Laser* module to improve object tracking.

¹We adopt 4 or 5 times up-sampling.

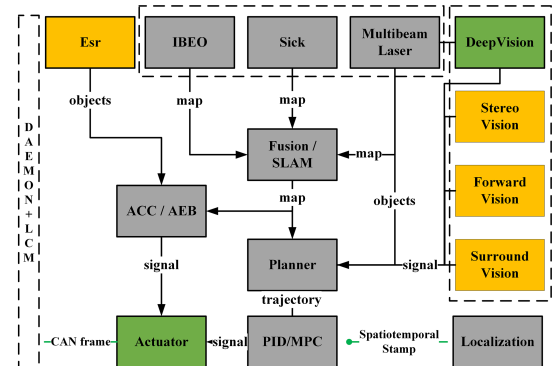


Fig. 3. The software architecture of TiEV

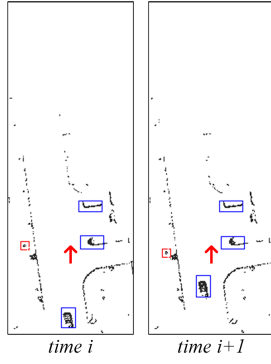


Fig. 4. The segmentation, classification and tracking of static and dynamic obstacles based on HDL64 (blue boxes indicate vehicles, red boxes indicate pedestrians, the red arrow represents the ego pos)

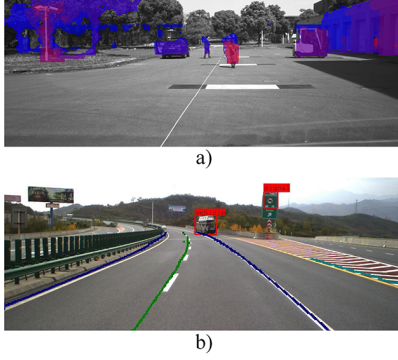


Fig. 5. The results of *forward vision module* (a) shows the depth map from stereo vision; b) shows the signal and vehicle detection and lane segmentation from deep vision)

2) *Surround vision*: TiEV also mounts four fisheye cameras. Based on the panoramic view (Fig. 6 a)), we propose an improved HFCN to segment parking spaces and lane markings [21]. The results are shown in Fig. 6 b).

C. Synchronization and Fusion

Notwithstanding our modules do not require hard synchronization as mentioned in Sec. II-B, multiple perceptual modules observe the surroundings in quite different frequencies. Their observation results should be aligned and fused.

Unlike pure timestamps based systems, which require a universal extrapolator to interpolate poses, we explicitly attached a pose information to messages in each sensory module once a measurement is made. This is realized by receiving a timely updated spatiotemporal stamp (t, x, y, θ) published by the *localization* module. The pose information will then be used to transform the observations to the current pose. The overall mismatch is about several centimeters, which is satisfied with driving even at relatively high speed. The time information in the stamp provides a constraint for the fusion, which ensures the latest observation is adopted.

To deal with possible false alarms from single sensor reading, a probabilistic fusion method of multiple sensors is employed. The fusion is performed in the overlapping region of measurements defined by the intersections of their field of

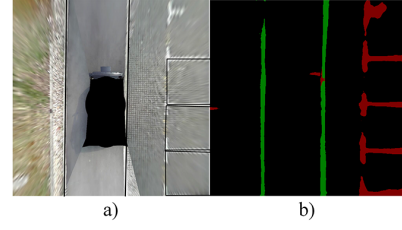


Fig. 6. Road marking extraction based on the surround vision system (a) the detected markings overlapped to the original image; b) the segmented results)

views in xy plane. A 2D virtual scan is firstly generated from *Multi-beam Laser* module to be aligned with *IBEO* and *Sick*. The occupancy grid-based representation is then adopted for the fusion of obstacles, in which the probability of a cell of being an obstacle is derived by:

$$\frac{p(x | z_{1:t})}{p(\bar{x} | z_{1:t})} = \prod_{k=1}^n \frac{p(x | z_t^k)}{p(\bar{x} | z_t^k)} \cdot \frac{p(x)}{p(\bar{x})} \cdot \frac{p(x | z_{1:t-1})}{p(\bar{x} | z_{1:t-1})}$$

where $p(x)$ is the state of being obstacle in one grid cell and $p(\bar{x})$ is its complementary. z_t^k indicate measurements of k sensors represented by *maps* from each module.

We choose a belief threshold of 0.75 to conservatively extract the maximum likelihood map (Fig. 7 a)). This fused map represents the drivable area closed to the vehicle [15]. Influences of noises, as well as false alarms, are drastically abbreviated. Finally, *map* of segmented obstacle from *Multi-beam Laser* module (Fig. 7 b)) and the historical *map* from SLAM modules (Fig. 7 c)) (described in Sec. IV) are merged to the grid cells of state unknown ($p(x) = 0.5$) from the previous step, which breeds the final fused map used in the *planner* module (Fig. 7 d)).

IV. INCREMENTAL MAPPING

With the local probabilistic fusion implemented above, it is naturally extended to mapping the historical map of the whole driving environment.

The state-of-the-art system, e.g., Cartographer [11], stored all the local maps and scans in memory, which can be burdensome when used in large-scale mapping. Alternately,

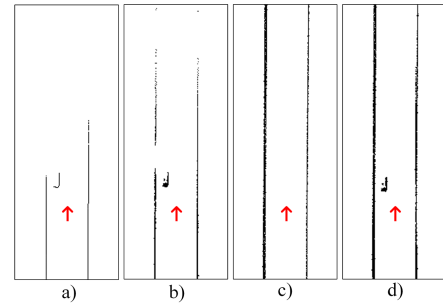


Fig. 7. The probabilistic fusion of laser detections (a) shows the fused drivable area from multiple sensors; b) shows the segmented obstacle from *Multi-beam laser*; c) shows the historical map of drivable area; d) shows the finally fused map for planning)

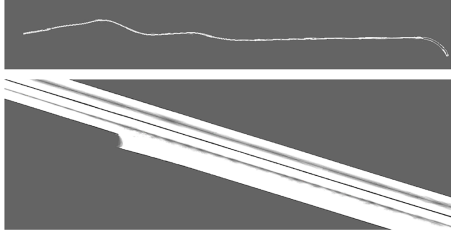


Fig. 8. The map of drivable area of 12km's long

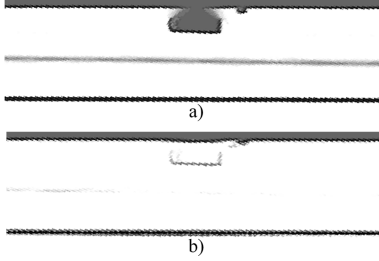


Fig. 9. The updating of the map of drivable area (a) shows a previously build map with a car parking on the road side; b) shows the updated result of the area in another day, where the influence of the car has been eliminated)

we take the usage of R-tree to index all the locally fused maps. Only the visible portion of the whole map will be kept in the memory while others are streamed out. In this way, we could map almost an area of arbitrary size. Fig. 8 shown a 12 km long path mapped using our method. The memory print is constantly bounded by around 150 MB.

In practice, the mapping of a large area could not be realized in one go, because of the limits of the battery or the traffic conditions during mapping. Therefore, we implemented an incremental mapping strategy thanks to the streaming design. When one mapping process finished, all the local maps are streamed onto disk. In the next run, our mapping module could load the surrounding previous maps and restore the mapping process. This mechanism brings the extra benefit of automatically map updating. We allow the overlapping between local maps, both spatially and temporally. When retrieving the visible maps during driving, we fused the surrounding overlapping local maps based on a weighted averaging strategy. The probability of a fused grid cell is derived from:

$$p(x) = \frac{1}{n} \sum_{i=1}^n w_i \cdot p(x_i)$$

where w_i is the weighting for the i th local map, which is given according to the date of acquisition. Fig. 9 shows a local map with a car parking on the roadside a), which is updated by the second round mapping in another day b).

V. THE 1ST AND 2ND PLANNING

We termed the path planning as the 1st planning and the trajectory planning as the 2nd planning because of their temporal relation. The 1st planning is only triggered when the current path cannot be continued, such as the road is blocked. The 2nd planning operates all the time when the

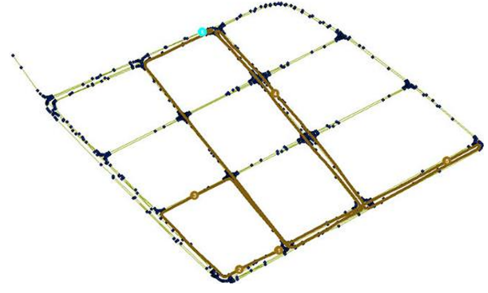


Fig. 10. The path planning results on the lane-based road network using pgRouting

vehicle is moving according to the path. We implement the less-frequent 1st planning in an open source spatial database system and implement a unified 2nd planning for both the structured and unstructured environment.

A. Path planning - The 1st planning

The 1st planning is based on HD maps captured by using our vehicle and edited using QGIS². All the lanes and intersections are sampled and topologically connected to form a lane-based road network. The road network also records path-related information such as the speed limits, the right of lane-change etc. We choose to manage the HD map with a spatial database rather than map files because such an HD map should be able to be accessed by multiple users simultaneous. We adopt the open-source spatial database PostGIS³, and use pgRouting⁴ to perform the shortest path finding (Fig. 10). This database-based implementation has a high performance and provides multiple accesses from multiple autonomous vehicles if the database is implemented remotely on a server.

B. Trajectory planning - The 2nd planning

TiEV introduces a unified planning module for both the structured and unstructured driving environment. An enhanced hybrid A* algorithm is used to find the optimal path on the grid-based representation considering the vehicle kinematics. We model the lanes, the static and dynamic obstacles, the parking space and the path from the 1st planning as weightings according to a unified weighting policy (Fig. 11). Several optimizations are proposed to bound the time expense of planning to within 20 to 80 milliseconds.

As a result, our unified planner could greatly simplify the FSM design in our decision-making engine. Moreover, it offers a more flexible and intelligent planning than conventional methods while TiEV is running on complex urban roads.

VI. THE SAFETY CONCERN

Safety is the highest priority of TiEV. We respect the safety of all traffic participants on road as well as the vehicle itself. The implementations will be described in car behavior and system design respectively.

²<https://www.qgis.org/>

³<http://www.postgis.net/>

⁴<http://pgrouting.org/>

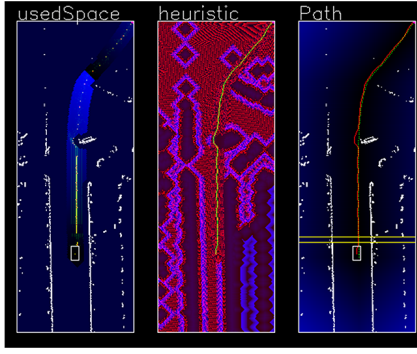


Fig. 11. The interface of TiEV's *planner* module, which shows a trajectory (the red dotted line) generated based on the obstacles as well as the path given by the 1st planning (the green dotted line)

A. Safety concern of TiEV's behavior

To our understanding, the utmost safety guarantee of an autonomous vehicle is to prevent active collision of the vehicle to any traffic participants, including pedestrians, cyclists, other vehicles, etc. This fatal behavior is tightly constrained in TiEV by the introduction of a dual ACC/AEB implementation.

The ACC/AEB function is implemented within two modules. The *planner* module, which is the brain of TiEV, calculates a safe speed v_{safe} in real time based on the distance to obstacles on the referenced path according to the following equation [7]:

$$v_{safe}(t) = v_{max}(1 - \exp(-\frac{c}{v_{max}}dist(t) - d))$$

where v_{max} is the highest permitted speed, $dist(t)$ is the distance between ACC/AEB target and current vehicle, c and d are model parameters. The target speed for the controller will then be restricted by both the speed limits and v_{safe} .

In the meantime, an independent ACC/AEB module is introduced and acts as a shadow planner, which bypasses the main planning module and directly communicates to the actuator module (Fig. 3). This module receives the fused map and the detected objects. The runtime steering angle and velocity are integrated to estimate a future trajectory according to current control states (Fig. 12). A safe speed is then calculated according to the previous equation. This speed limit is combined finally in the actuator module to further restrict the target speed even when the planner module is inoperative.

We run the module on two different computers to increase the redundancy. The above implementations are the main safeguard of TiEV during on-road driving. And we seldom collide with any static or moving objects during our experiments.

B. Safety concern of TiEV's system

Autonomous cars will eventually carry families, driving on real roads every day [14]. Almost any system faults will not be tolerated, especially those related to the core functionality. Although TiEV is designed as an experimental prototype, we make the design to fulfill the systematic safety requirements.

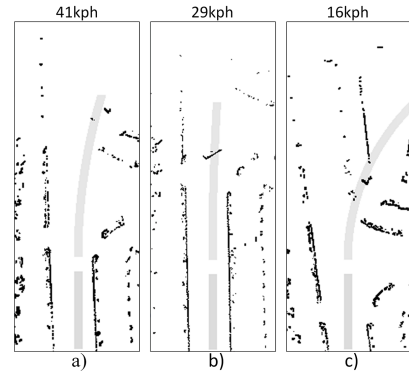


Fig. 12. The v_{safe} calculated by ACC/AEB module (top line), where the gray zone represents the predicted path based on current control states

The daemon modules that listen to heartbeats of all other modules are implemented redundantly. On a local computer, a daemon module tries to restart local modules that no longer sending out heartbeats or sending out heartbeats with frozen spatiotemporal stamps. Remotely, the heart beats of daemon modules are also monitored by each other from separate computers. Once a daemon module is judged as a failure, it means the computer or the networking service has failed. In this case, TiEV will try to stop the vehicle immediately. To guarantee the robust communication between computers and the vehicle, we also introduce redundant CAN communication interfaces. Another CAN interface is installed on one IPC as the backup. Both computers could monitor and send CAN messages independently.

In practice, TiEV system has an extremely low probability of failure. One can even introduce redundancy to computers to further decrease the risks.

VII. EXPERIENCES GAINED FROM THE FUTURE CHALLENGE

The on-road competition of the IVFC is composed of two events, i.e., the express road competition and the urban road competition (Fig. 13). The exact task points of both events are not released until 30 minutes before the competition. As a result, the participants have to build their own roadmap in advance. In the competitions, vehicles have to recognize various situations on the road, e.g., signals, blockages, tunnels, pedestrians, other vehicles etc. and behave properly. The final score will be given based on evaluations of the task achievements, the traffic violations, and the time costs.

Our main experiences gained can be laid in three-folds:

The first is the lack of ability of comprehensive perception. TiEV could recognize traffic signals, three kinds of traffic participants as stated in Sec. III, but it treats others simply as obstacles. This cause problems when coming across specific scenes containing barriers made by e.g., reflective triangles or cones, which warn the driver of blockages located ahead.

Secondly, the tight coupling of autonomous driving and high precise lane-based map can be problematic if the map is erroneous because of, e.g., simply out of date. The using of the lane-based map also demands highly precise localization.



Fig. 13. TiEV in the IVFC

Our planning module is designed not to be exactly relying on the lane-based path (which however is the case for many others, who directly generate trajectories based on the path). TiEV treats the path as one of the references as the detected lanes and obstacles (Sec. V-B). Nevertheless, a path shifted meters from the correct position still cause problems.

Finally, TiEV employs cascade controller to faithfully follow the trajectory output from the 2nd planning. It will abruptly turn the wheel when the consequent trajectories are not smoothly connected, e.g., when the 2nd planning suddenly switches from one trajectory to another. This results in an agile but uncomfortable riding experience. To abbreviate this effect, we introduce a piecewise planning strategy that keeps a local window of trajectory constant and concatenates the following trajectory smoothly at the point beyond the look-ahead region. In practice, this method successively stabilizes the vehicle when driving up to 60kph (the highest speed limit of IVFC) with our free-style planner.

VIII. CONCLUSION REMARKS

We clearly realized that the ability of TiEV is still far from what is demanded for realistic applications on complex urban roads. The system could already cope with many scenarios and drive the vehicle safely. Nevertheless, it still cannot match up to human drivers in respect of adaptivity to environmental variations and robustness when facing noises.

Deep learning-based methods have greatly strengthened the capability of perception. However, such perception still lacks the ability to understand the contextual semantics of driving, such as the relations and interactions between traffic participants in a driving environment. This can only be realized with the help of the memory or the modeling of driving experiences. Besides, the online perception burden can easily surpass the onboard computing resources. Human driver relieves this burden by emphasizing on specific objects according to current driving intentions, which is known as the attention mechanism. This calls for a tighter coupling between the planning and the perception functions. Moreover, human drivers usually do not have to behave "optimally" as algorithms do. Planning optimization should, therefore, be relaxed for temporally suboptimal solutions and should be regularized to react robustly to disturbances.

At last, we argue that the technical route of autonomous driving is still under drastic evolution. Differentiations of implementations worldwide will eventually benefit to the maturation of the autonomous driving systems.

ACKNOWLEDGMENT

Special thanks to Deyi Li, Wei Han, Changzhu Zhang, Lifeng An, Jing Zhu and Peizhi Zhang for the provided helps and discussions during the implementations.

REFERENCES

- [1] M. Aeberhard, S. Rauch, M. Bahram, G. Tanzmeister, J. Thomas, Y. Pilat, F. Himm, W. Huber, and N. Kaempchen, "Experience, results and lessons learned from automated driving on germany's highways," *IEEE Intelligent Transportation Systems Magazine*, vol. 7, no. 1, pp. 42–57, 2015.
- [2] C. Berger and B. Rump, "Autonomous driving - 5 years after the urban challenge: The anticipatory vehicle as a cyber-physical system," *ArXiv e-prints*, 2014.
- [3] J.-F. Bonnefon, A. Shariff, and I. Rahwan, "The social dilemma of autonomous vehicles," *Science*, vol. 352, no. 6293, pp. 1573–1576, 2016.
- [4] A. Broggi, P. Cerri, S. Debatisti, M. C. Laghi, P. Medici, M. Panciroli, and A. Prioletti, "Proud-public road urban driverless test: Architecture and results," in *2014 IEEE Intelligent Vehicles Symposium Proceedings*, June 2014, pp. 648–654.
- [5] A. Broggi, S. Debatisti, P. Grisleri, and M. Panciroli, "The deeva autonomous vehicle platform," pp. 692–699, June 2015.
- [6] M. Buechel, J. Frtunikj, K. Becker, S. Sommer, C. Buckl, M. Armbruster, A. Marek, A. Zirkler, C. Klein, and A. Knoll, "An automated electric vehicle prototype showing new trends in automotive architectures," in *2015 IEEE 18th International Conference on Intelligent Transportation Systems*, Sept 2015, pp. 1274–1279.
- [7] C. Chen, A. Seff, A. Kornhauser, and J. Xiao, "Deepdriving: Learning affordance for direct perception in autonomous driving," in *2015 IEEE International Conference on Computer Vision (ICCV)*, Dec 2015, pp. 2722–2730.
- [8] A. Cosgun, L. Ma, J. Chiu, J. Huang, M. Demir, A. M. Anon, T. Lian, H. Tafish, and S. Al-Stouhi, "Towards full automated drive in urban environments: A demonstration in gomentum station, california," *ArXiv e-prints*, 2017.
- [9] DMV, "Autonomous vehicles in california," DMV, Tech. Rep., 2016.
- [10] D. Dolgov, S. Thrun, M. Montemerlo, and J. Diebel, "Path planning for autonomous vehicles in unknown semi-structured environments," *The International Journal of Robotics Research*, vol. 29, no. 5, pp. 485–501, 2010.
- [11] W. Hess, D. Kohler, H. Rapp, and D. Andor, "Real-time loop closure in 2d lidar slam," in *2016 IEEE International Conference on Robotics and Automation (ICRA)*, ser. 2016 IEEE International Conference on Robotics and Automation (ICRA), 2016, pp. 1271–1278.
- [12] A. S. Huang, E. Olson, and D. C. Moore, "Lcm: Lightweight communications and marshalling," in *2010 IEEE/RSJ International Conference on Intelligent Robots and Systems*, ser. 2010 IEEE/RSJ International Conference on Intelligent Robots and Systems, 2010, pp. 4057 – 4062.
- [13] L. Li, W. L. Huang, Y. Liu, N. N. Zheng, and F. Y. Wang, "Intelligence testing for autonomous vehicles: A new approach," *IEEE Transactions on Intelligent Vehicles*, vol. 1, no. 2, pp. 158–166, June 2016.
- [14] M. Maurer, J. C. Gerdes, B. Lenz, and H. Winner, *Autonomous Driving Technical, Legal and Social Aspects*. Springer, Berlin, Heidelberg, 2016.
- [15] M. Montemerlo, J. Becker, S. Bhat, H. Dahlkamp, D. Dolgov, S. Ettinger, D. Haehnel, T. Hilden, G. Hoffmann, B. Huhne, and Others, "Junior: The stanford entry in the urban challenge," *Journal of field Robotics*, vol. 25, no. 9, pp. 569–597, 2008.
- [16] J. Redmon and A. Farhadi, "YOLO9000: Better, Faster, Stronger," *ArXiv e-prints*, 2016.
- [17] I. Shim, J. Choi, S. Shin, T. H. Oh, U. Lee, B. Ahn, D. G. Choi, D. H. Shim, and I. S. Kweon, "An autonomous driving system for unknown environments using a unified map," *IEEE Transactions on Intelligent Transportation Systems*, vol. 16, no. 4, pp. 1999–2013, 2015.
- [18] A. Teichman and S. Thrun, "Tracking-based semi-supervised learning," *The International Journal of Robotics Research*, vol. 31, no. 7, pp. 804–818, 2012.

- [19] C. Urmson, J. Anhalt, D. Bagnell, C. Baker, R. Bittner, M. N. Clark, J. Dolan, D. Duggins, T. Galatali, C. Geyer, M. Gittleman, S. Harbaugh, M. Hebert, T. M. Howard, S. Kolski, A. Kelly, M. Likhachev, M. McNaughton, N. Miller, K. Peterson, B. Pilnick, R. Rajkumar, P. Rybski, B. Salesky, Y.-W. Seo, S. Singh, J. Snider, A. Stentz, W. R. Whittaker, Z. Wolkowicki, and J. Ziegler, "Autonomous driving in urban environments: boss and the urban challenge," *Journal of Field Robotics*, vol. 25, no. 8, pp. 425–466, 2008.
- [20] Waymo, "On the road to fully self-driving," Waymo, Tech. Rep., 2017.
- [21] T. Yang, Y. Wu, J. Zhao, and L. Guan, "Semantic segmentation via highly fused convolutional network with multiple soft cost functions," *arXiv preprint arXiv:1801.01317*, 2018.
- [22] J. Ziegler, P. Bender, M. Schreiber, H. Lategahn, T. Strauss, C. Stiller, T. Dang, U. Franke, N. Appenrodt, C. Keller, and Others, "Making bertha drive - an autonomous journey on a historic route," *IEEE Intelligent Transportation Systems Magazine*, vol. 6, no. 2, pp. 8–20, 2014.